Research Article

Hanjiang Wu, Tao Huang*, Kexing Song*, Yanmin Zhang*, Yanjun Zhou, Shaolin Li, and Xin Li

Study on deformation characteristics of multipass continuous drawing of micro copper wire based on crystal plasticity finite element method

https://doi.org/10.1515/ntrev-2023-0110 received May 12, 2023; accepted August 1, 2023

Abstract: Copper-based wire has excellent comprehensive performance and is widely used in integrated circuit packaging, electronic communication, connectors, audio and video transmission, and other fields. Based on the crystal plasticity finite element method, the crystal plasticity finite element model of multi-pass continuous drawing deformation of pure copper micro wires was established, and the reliability of the model was proved. The continuous drawing deformation behavior of micro wires under high-speed deformation and micro wire diameter scale effect was studied. The research shows that there is a fracture risk zone under the alternating action of positive and negative stress values in the deformation zone of the drawn wire. The changing drawing force and contact stress during the continuous drawing process of the wire will also reduce the stability and surface quality of the wire during the drawing process. The shear deformation and slip degree of the surface grain of the drawn wire are greater than those of the core grain, and the drawing die has a greater impact on the slip system state of the surface of the wire. With the increase in drawing passes, the mechanical characteristics inside the wire increase accordingly, and the deformation uniformity inside the grains is improved. The established model can demonstrate the

Keywords: crystal plasticity, finite element, copper, micro wire, drawing deformation

1 Introduction

The processing of wire has gone through two processes: the preparation of continuous casting rod billets and the continuous drawing deformation of wire. The multi-pass continuous drawing deformation process is the most important link that impacts the comprehensive performance of wire. With the rapid development of the electronic industry and communication technology, in recent years, electronic devices have rapidly developed towards high integration and miniaturization, which has present higher demands for the comprehensive performance of wire, such as high conductivity and high elongation. The process performance is developing towards ultrafine, ultra-long, and ultra-precision, and the demand for micro wires in the field of integrated circuits has been increasing. The micron-scale wire drawing process and the mechanical behavior of materials at the micro-nano scale have attracted more and more attention, and also put forward a huge demand for large-scale manufacturing of micro parts [1–3].

In recent years, many scholars have conducted research on the microstructure, properties, and macroscopic mechanical behavior of copper wire. Hanazaki *et al.* [4] prepared copper wire with ultra-fine grain structure and high strength by multiple-pass deep drawing. Sun *et al.* [2] found that oxygen-free copper wire exhibited simultaneous improvements in strength and conductivity at the late stage of cold drawing deformation, which was possibly attributed to the formation of fine elongated grains inside the wire. Yang *et al.* [5,3] discovered that the microstructure inside low-oxygen copper wire gradually fibrously transformed with increasing deformation, forming a <001> and <111> fiber texture. Chen and Huang [6] studied the mechanical behavior of brass alloy wire during the drawing process using rigid-plastic finite

Hanjiang Wu, Yanjun Zhou, Shaolin Li, Xin Li: School of Materials Science and Engineering, Henan University of Science and Technology, Luoyang 471023, China

deformation history characteristics and structure inheritance of the continuous wire drawing process.

^{*} Corresponding author: Tao Huang, School of Materials Science and Engineering, Henan University of Science and Technology, Luoyang 471023, China, e-mail: huangtao@haust.edu.cn

^{*} Corresponding author: Kexing Song, School of Materials Science and Engineering, Henan University of Science and Technology, Luoyang 471023, China; Henan Academy of Sciences, Zhengzhou, 450000, China, e-mail: kxsong@haust.edu.cn

^{*} Corresponding author: Yanmin Zhang, School of Materials Science and Engineering, Henan University of Science and Technology, Luoyang 471023, China, e-mail: zhangmin70@163.com

element and optimized process parameters. Chang *et al.* [7] established the strain—hardness relationship model of copper wire and used finite element simulation to predict the hardness of copper wire drawing. The model was found to be suitable for small deformation copper wire drawing. Celentano [8] developed a thermodynamic simulation model of copper wire drawing process, which proved to be effective in predicting the mechanical and thermodynamic behaviors of copper wire during drawing. Tang *et al.* [9] studied the evolution of damage during multi-pass wire drawing process and found that the damage value inside the wire continuously increased with the increase in the drawing passes and exhibited nonlinear characteristics.

When the size of the formed metal parts is reduced to the micro scale, the forming process, mechanical behavior, and performance of the material are obviously different from those at the macro scale [10,11]. The differences in part size and grain microstructure can lead to anisotropy in flow stress and plastic deformation, resulting in the so-called size effect [12–14]. At this time, micro-scale material can no longer be regarded as a uniform continuum like in the macro-scale, which makes the traditional classical plastic theory based on continuum hypothesis and macro-phenomenological experiments unable to be directly applied to microforming research [15,16]. Therefore, it is necessary to use appropriate models for numerical analysis, and the crystal plastic finite element technology that has gradually developed in recent years undoubtedly becomes a good means to solve these problems.

In summary, the current research on wire deformation processing primarily focuses on larger wire diameters and conventional drawing conditions [17–19]. However, the micro-deformation mechanism of the continuous drawing process of micro copper wire under high-speed deformation conditions remains unclear and requires further exploration. This study presents a two-dimensional crystal plasticity finite element model of pure copper micro wire drawing. Using Abaqus finite element software, we simulated and analyzed the deformation history characteristics and heredity of the three-pass continuous drawing process of pure copper micro wire. We also studied in detail the influence of drawing passes on the non-uniform deformation and slip evolution of pure copper micro wire drawing process.

2 Theory of crystal plasticity mechanics

The crystal will produce elastic deformation and plastic deformation under the action of deformation force, and these two deformation modes are carried out simultaneously. Therefore, the total deformation gradient F is composed of plastic deformation gradient F^p caused by dislocation slip in the crystal and elastic deformation gradient F^e caused by lattice distortion and rotation in the crystal [20,21].

$$F = F^e F^p. (1)$$

where F^p is the plastic deformation gradient in the process of crystal deformation [22], and its derivative with respect to time is expressed as follows:

$$\dot{F}^p = \sum_{\alpha=1}^N \dot{y}^\alpha m^\alpha \otimes n^\alpha. \tag{2}$$

where m^{α} and n^{α} are the unit vectors of the slip direction and the normal direction of the slip surface before the deformation of the slip system α , respectively. $\dot{\gamma}^{\alpha}$ is the slip shear strain rate on the slip system α [23] and is expressed as follows:

$$\dot{y}^{\alpha} = \dot{y}_{0}^{\alpha} \left| \frac{\tau^{\alpha}}{g^{\alpha}} \right|^{n} \operatorname{sgn}(\tau^{\alpha}) \quad \tau^{\alpha} \ge \tau_{c}^{\alpha}, \tag{3}$$

$$\dot{y}^{\alpha} = 0 \quad \tau^{\alpha} < \tau_{c}^{\alpha}, \tag{4}$$

where n is the strain rate sensitivity coefficient of the slip system; \dot{y}_0^a is the reference shear strain rate of slip system α ; τ^a is the shear stress of slip system α ; and g^a is the critical shear stress of slip system α . The critical shear stress rate \dot{g}^a can be expressed as follows:

$$\dot{g}^{\alpha} = \sum_{\beta=1}^{N} h_{\alpha\beta} |\dot{\gamma}^{\beta}|,\tag{5}$$

where $h_{\alpha\beta}$ is the hardening coefficient of the slip system. the ratio of the latent hardening coefficient $h_{\alpha\beta}(\alpha \neq \beta)$ to the self-hardening coefficient $h_{\alpha\alpha}(\alpha = \beta)$ is generally taken as 1–1.5. The relationship between them is expressed as follows [24–26]:

$$h_{\alpha\beta} = qh_{\alpha\alpha} \quad (\alpha \neq \beta), \tag{6}$$

$$h_{\alpha\alpha} = h_0 \operatorname{sec} h^2 \left| \frac{h_0 \gamma}{\tau_s - \tau_0} \right|, \tag{7}$$

where h_0 is the initial hardening modulus, τ_s is the saturation value of the critical shear stress, and τ_0 is the critical value of the initial shear stress. The cumulative shear strain γ of all slip systems is expressed as follows:

$$\gamma = \sum_{\alpha=1}^{N} \int_{0}^{t} |\dot{\gamma}^{\alpha}| dt.$$
 (8)

3 Establishment and verification model

3.1 Experimental materials

Pure copper rod billet with a diameter of 16 mm was prepared by horizontal continuous casting equipment, and then micro copper wire with a diameter of 180 µm was obtained by multipass continuous drawing process. In order to observe the microstructure inside the wire, transmission electron microscope (TEM) characterization experiments are needed. The analysis sample was cut from the longitudinal section of the wire, and the TEM sample was prepared by double spray electrolytic polishing, and then TEM observation was performed under the FEI Talos F200X TEM. Figure 1 is the TEM image of 180 µm micro copper wire. From the diagram, it can be seen that after multi-pass continuous drawing deformation of pure copper wire, the grains inside the wire are obviously elongated in the drawing direction. There is a large quantity of dislocations inside the grains, and the dislocations are entangled with each other inside some grains to form high-density dislocations.

3.2 Model establishment

The micro wire studied in this work is a pure copper material with a face-centered cubic crystal structure, and its

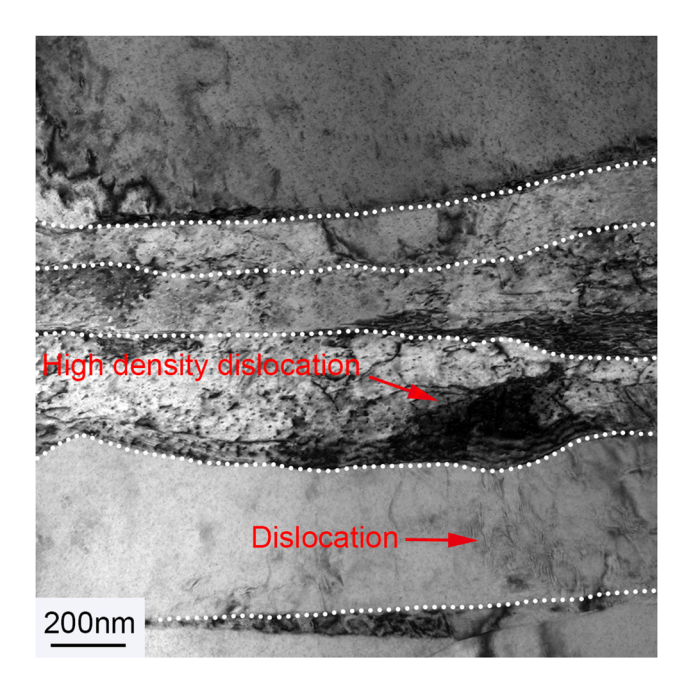


Figure 1: TEM image of micro copper wire.

elastic modulus is G11 = 168.4 GPa, G22 = 121.4 GPa, and G22 = 75.4 GPa. The dislocation slip motion during the plastic deformation process of pure copper material is carried out on the {111} (110) slip system, and the definition of the slip system is shown in Table 1 [27]. In order to conduct subsequent simulation work, it is necessary to determine the constitutive parameters of the material. A set of hardening parameters were obtained by fitting the stressstrain curves obtained by experiments and simulations of the tensile process of micro copper wires: $h_0 = 90$, $\tau_s = 54$, τ_0 = 12, n = 10, and $\dot{\gamma}_0$ = 0.001. Figure 2 is the stress–strain curve of the tensile process of the micro copper wire obtained by the tensile tester and the crystal plasticity simulation. It can be seen that the stress-strain curves obtained by the experiment and the simulation are in good agreement, that is, the material constitutive model is completed.

Based on the plane strain assumption [28], the crystal plasticity finite element model of multi-pass continuous drawing of micro copper wire was established. The Xaxis is set to the drawing direction, the Y axis is set to the normal direction, and the Z axis is set to the transverse direction. The schematic diagram and coordinate setting of the multi-pass continuous drawing process of micro copper wire are shown in Figure 3. In actual production, the multipass continuous drawing process of micron copper wire is carried out under the condition of high-speed deformation. The convergence of the established crystal plasticity model is a challenge under the interaction of high-speed deformation process conditions and micro-diameter size effects. In this study, the convergence of the calculation results is finally achieved by adjusting the incremental step and the contact between the drawing die and the wire. The initial incremental step is set to 3×10^{-7} , the contact pressure is 0.001, and the contact gap is 0.0001. In the preprocessing setting of the crystal plastic finite element model of the multi-pass continuous drawing process of the micro copper wire, the micro copper wire and the

Table 1: Slip system in the established crystal plasticity finite element model

Slip system	Slip direction	Slip plane	•	Slip direction	Slip plane
a1	[0 1 1]	(1 1 1)	b1	[1 0 1]	(1 1 1)
a2	$[1 \ 0 \ \overline{1}]$		b2	[1 1 0]	
a3	$[\overline{1} \ 1 \ 0]$		b3	$[0 \ \overline{1} \ 1]$	
c1	[0 1 1]	$(1 \overline{1} 1)$	d1	[0 1 1]	$(1 \ 1 \ \overline{1})$
c2	[1 1 0]		d2	[1 0 1]	
c3	$\begin{bmatrix} 1 & 0 & \overline{1} \end{bmatrix}$		d3	$[\overline{1} \ 1 \ 0]$	

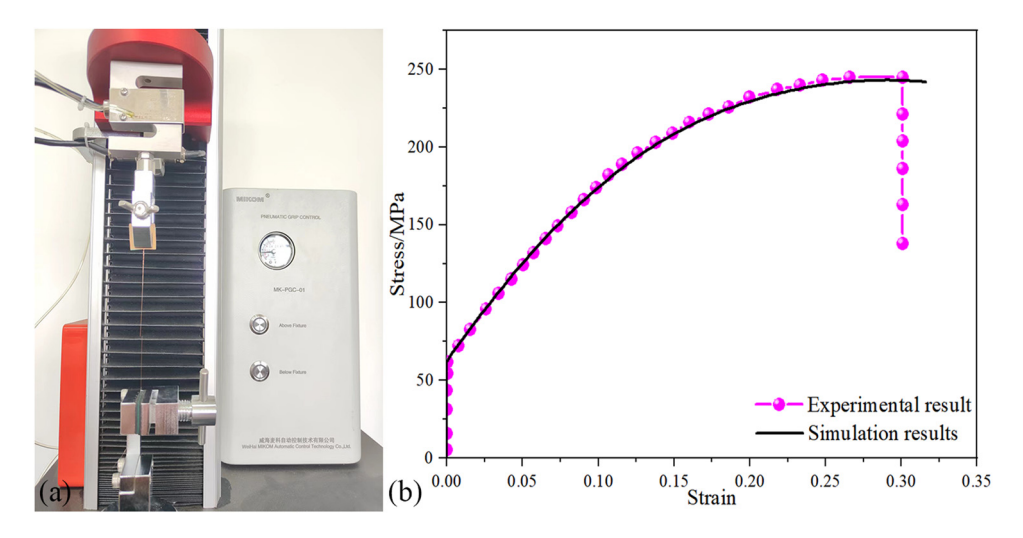


Figure 2: (a) Tensile tester and (b) comparison of stress–strain curves obtained by tensile test and crystal plasticity finite element of micro copper wire.

drawing die are set as deformable bodies and rigid bodies, respectively. In order to better ensure the convergence of the calculation results, the model was divided into regular quadrilateral meshes, and finally the model was discretized by CPE4R element. The process parameters of multi-pass continuous drawing process of micro copper wire mainly include drawing speed and friction coefficient between the drawing die and the wire. The drawing process parameters of micro copper wire are set as follows: the drawing speed is 1 m/s, the friction coefficient between the drawing die and the wire is 0.07, and the wire diameter compression rate is 10%.

In order to accurately reflect the initial crystal orientation inside the sample in the established crystal plasticity finite element model, 200 representative grain orientations were extracted from the EBSD results of the longitudinal section of the 180 μ m micro copper wire to complete the initial orientation assignment of the grains inside the model. Then, according to the strip grain shape information obtained

from the experiment, the construction of the micro copper wire model can be completed. Figure 4 is the crystal plasticity finite element model of 180 μ m micro copper wire. The grain shape in the figure is elongated and assigned the crystal orientation obtained from the EBSD results. In order to obtain some key information during the wire drawing process, three tracking points A, B, and C were marked in the upper surface, core, and lower surface grains of the wire.

3.3 Model validation

Based on the obtained crystal plasticity parameters, the drawing process of micro pure copper wire from 320 to 180 μ m was simulated. Figure 5 is a comparison of the {111} pole figures obtained by experiment and crystal plasticity simulation. It can be seen from the diagram that after the drawing deformation of the pure copper wire, $\langle 111 \rangle$

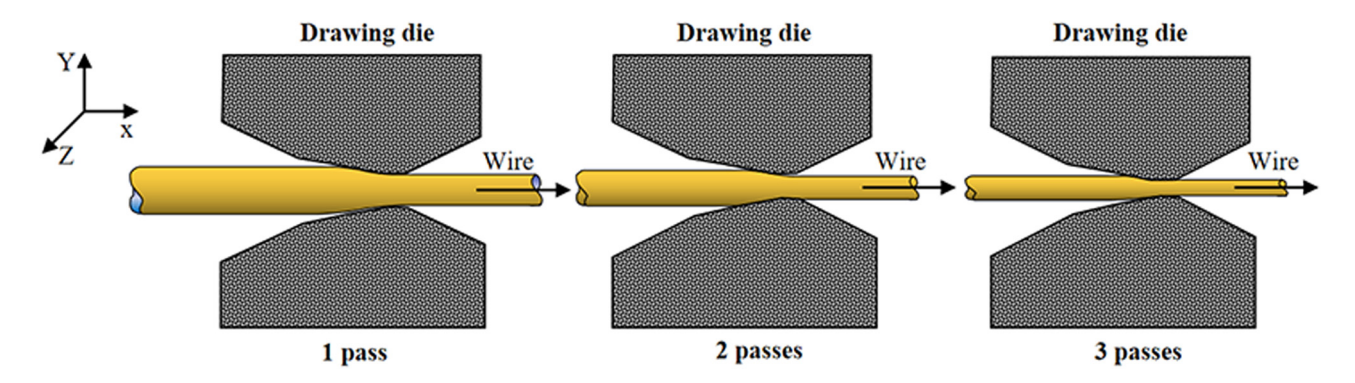


Figure 3: Multi-pass continuous drawing diagram of wire.

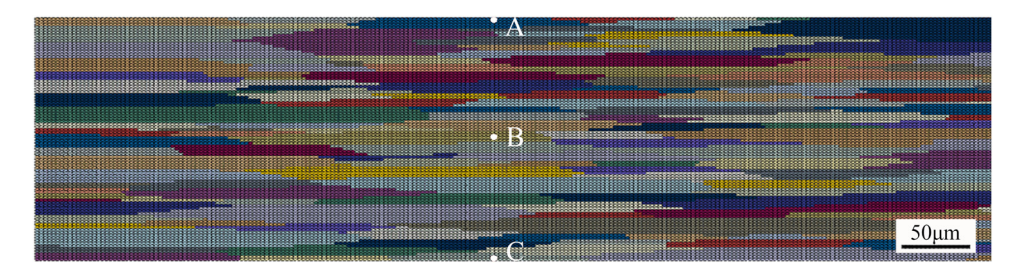


Figure 4: Crystal plastic finite element model of micro copper wire.

fiber texture is formed inside the wire. It shows that in the process of wire drawing deformation, most of the grains inside the wire rotate to the $\langle 111 \rangle$ direction under the action of intergranular interaction and drawing force. The pole figures obtained by the EBSD experimental results and the crystal plasticity finite element simulation results are in good agreement, which verifies the accuracy of the crystal plasticity finite element model for micro pure copper wire drawing.

4 Results and discussion

Figure 6 shows the change in drawing force during threepass continuous drawing of micro copper wire. From the diagram, it can be seen that the drawing force is not a stable value in the wire drawing process. When the wire just contacts the drawing die, the drawing force increases rapidly in a short time, and then the wire enters a stable drawing stage with a certain fluctuation. When the wire passes through the drawing die completely, the drawing force decreases rapidly to 0. First, with the increase in

continuous drawing passes, the strength and hardness of the copper wire continue to increase, indicating the occurrence of work hardening phenomenon. Therefore, more energy is needed to overcome the hardness and strength of the material during the drawing process. However, in the process of larger plastic deformation, the deformed copper structure is also prone to dynamic recovery and recrystallization. However, under the current wire diameter compression rate of 10% per pass and the cumulative deformation degree of three consecutive passes, the effect of work hardening on the drawing force still plays a major role, which leads to the increase in wire drawing force with the increase in drawing passes. Therefore, the state of drawing force during the continuous drawing process of copper wire is a result of the combined effects of competitive mechanical phenomena such as work hardening, dynamic recrystallization, dynamic recovery, frictional force, and temperature rise during plastic deformation process. When the wire is deformed to a certain extent, the growth rate of the drawing force may be inhibited, showing a trend of increasing first and then slowly increasing or then decreasing, which is similar to the trend of rolling force in the multi-pass rolling process [29]. The

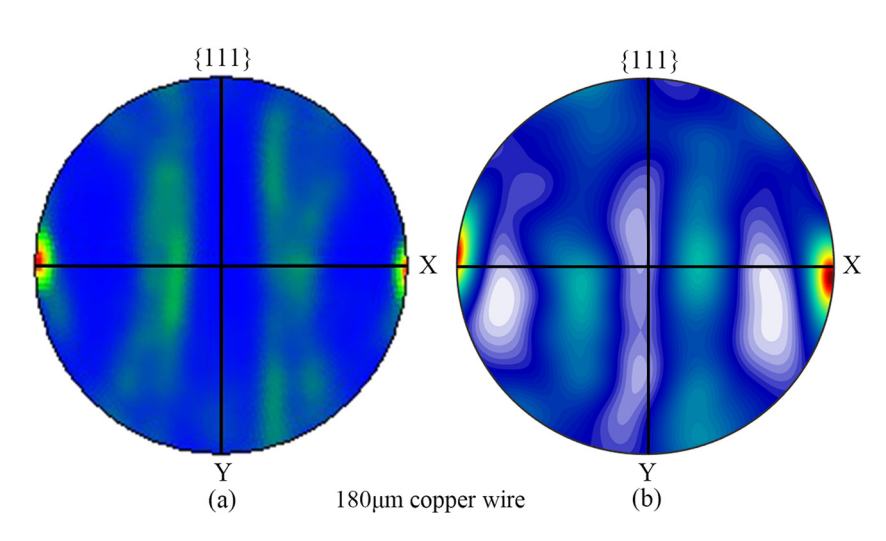


Figure 5: Comparison of simulated and experimental (111) pole figures: (a) experiment and (b) simulation.

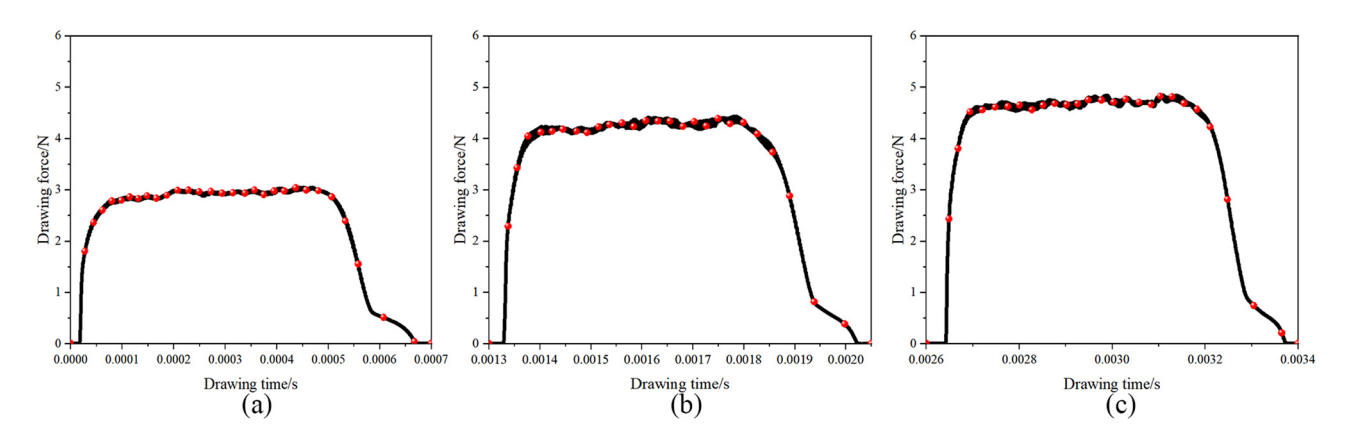


Figure 6: The relationship between drawing force and drawing time during multi-pass continuous drawing of wire: (a) one pass, (b) two passes, and (c) three passes.

drawing time of each pass also increases with the drawing process. This is because with multiple passes of drawing deformation, the accumulated deformation of the wire increases to a certain degree, resulting in a larger plastic deformation of the wire and making it thinner and longer. As a result, the time required to complete the deformation for each drawing pass also increases accordingly.

The stability of the wire drawing process and the surface quality of the drawn wire are not only affected by the drawing force in the drawing direction, but also by the contact stress between the drawing die and the wire.

Figure 7 shows the variation in the contact stress between the upper and lower surfaces of the micro copper wire and the drawing die with time during the three-pass continuous drawing process. Here the contact pressure and friction stress are collectively referred to as the contact stress between the wire and the drawing die. From the diagram, it can be observed that there are certain differences and fluctuations in the contact stress state between the upper and lower surfaces of the wire and the drawing die. This is caused by variations in the grain structure, grain orientation, and number of grain boundaries between the upper

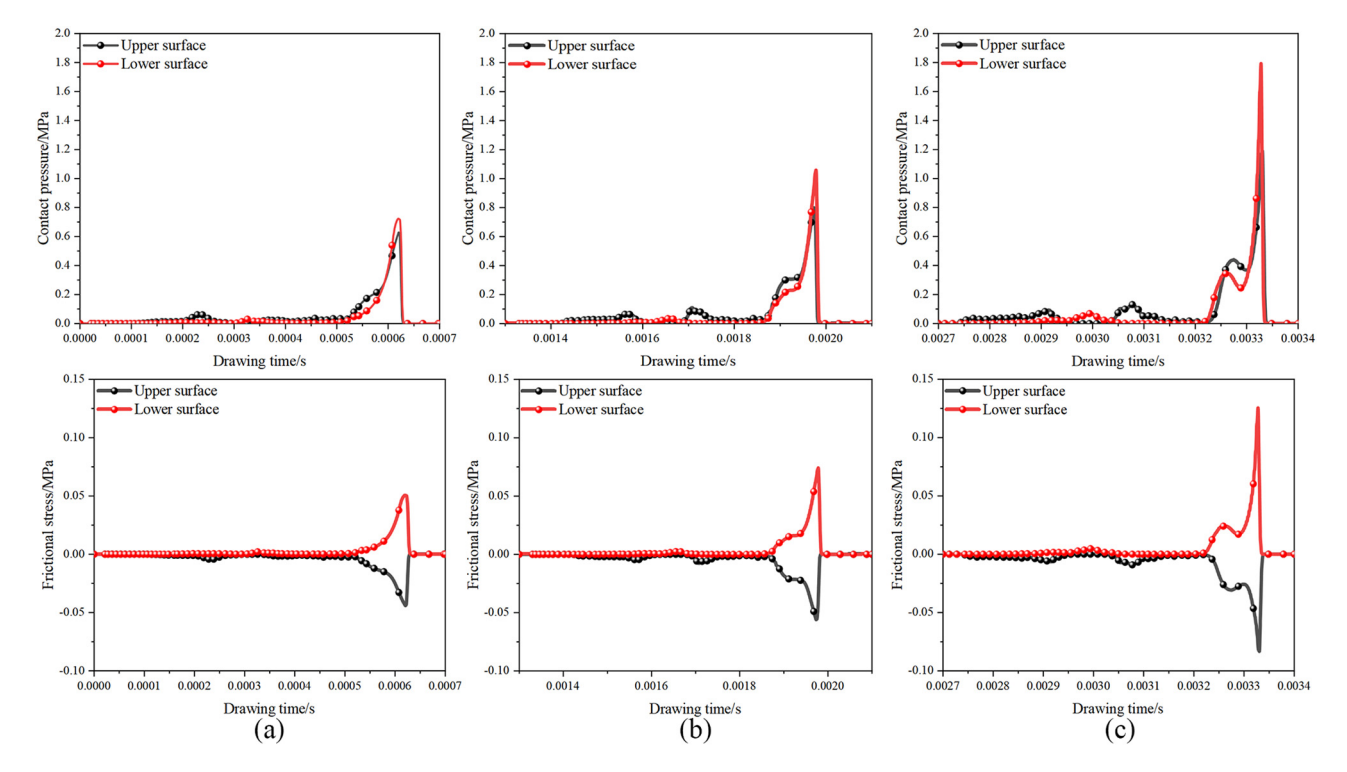


Figure 7: The change in contact stress with time during multi-pass continuous drawing of wire: (a) one pass, (b) two passes, and (c) three passes.

and lower surfaces of the wire. During the drawing process, the contact pressure and frictional stress on the upper and lower surfaces of the wire are in the same and opposite directions, respectively. In the early stages of the wire drawing process, the wire surface is in a low stress state with fluctuations. As the drawing process progresses, the contact stress on the wire surface increases significantly within a certain distance before the wire exits the drawing die. After the wire leaves the drawing die, the contact stress on the wire surface rapidly decreases and eventually reaches 0. This is because when the wire is about to leave the drawing die, the part of the wire that has already been drawn is longer, and the part of the wire that has not been drawn is shorter. These two parts present a "top heavy" stress imbalance on both sides of the drawing die, and as the drawing process progresses, the contact between the wire surface and the die surface will also suddenly decrease. With the increase in drawing passes, the contact stress on the wire surface has been improved, and this fluctuating contact stress state has caused additional deformation characteristics on the wire surface. After multi-pass deformation accumulation, the wire surface will exhibit a certain level of roughness after the final drawing.

Figure 8 shows the stress distribution in the drawing deformation zone of micro copper wire during three-pass continuous drawing. From the diagram, it can be seen that the deformation inside the drawn wire is uneven. There is

a significant stress gradient phenomenon inside the wire that passes through the sizing strip of the drawing die, and a high-stress concentration area appears on the surface, as shown in the red area. The stress value gradually decreases from the surface to the center of the wire. Additionally, the inclined surface of the wire that contacts the compression surface of the drawing die to the center also shows a state of stress gradient. Specifically, the surface exhibits a higher negative stress, while the center manifests a higher positive stress. Under the alternating action of positive and negative stress values, the fracture risk of the wire during the drawing process increases. When the drawing pass increases, the increase in the cumulative deformation of the drawn wire result in the increase in the stress value and the non-uniformity of the deformation area of the drawn wire, and the area of the high-stress concentration area gradually increases. The high-stress concentration area includes the surface of the wire that passes through the sizing strip of the drawing die and the surface and core area of the wire that contacts the compression surface of the drawing die. Figure 9 shows the relationship between the stress of the marked points in the drawing deformation zone of the micro copper wire and the drawing time during the three-pass continuous drawing process. The marked points A, B, and C are located on the upper surface, core, and lower surface of the wire in Figure 4, respectively. From the diagram, it can be seen that the stress states at

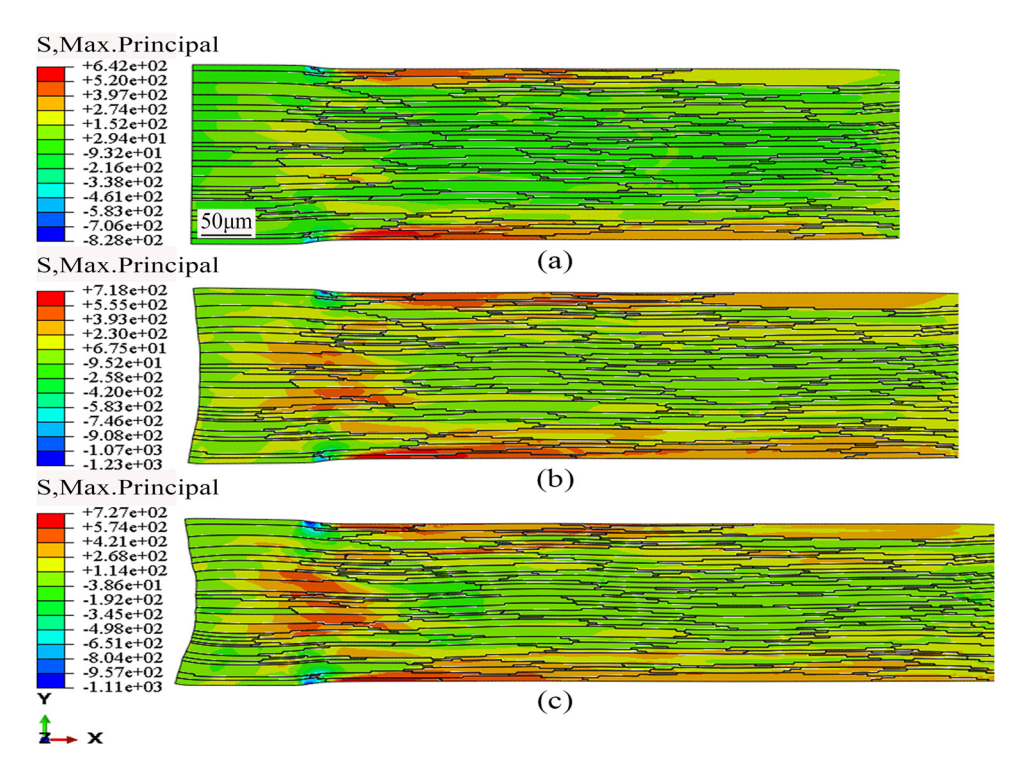


Figure 8: The stress distribution in the drawing deformation zone of wire in different passes: (a) one pass, (b) two passes, and (c) three passes.

8 — Hanjiang Wu et al. DE GRUYTER

different positions inside the wire are different during the drawing process. With the drawing process, when the internal marked points of the drawn wire undergo deformation, positive and negative alternating stress fluctuations are observed at different marked points within the wire. This is because the deformation of different regions in the same grain is not uniform, and the deformation of adjacent grains is also coordinated with each other, which causes the stress field around the marked points inside the wire change continuously during the drawing process, which leads to the occurrence of stress fluctuation during the wire drawing process. Among them, the stress fluctuation of the upper and lower surface positions of the drawn wire is more severe than that of the core position. Since the marked points A, B, and C are located on the same vertical line inside the wire, when the drawing deformation is just on the surface of the wire above the marked point, the three marked points will reach their respective maximum principal stress state at almost the same time. With the increase in drawing passes, the average stress at different positions of the longitudinal section of the drawn wire shows an increasing trend, which indicates that with the continuous drawing process of multiple passes, not only the surface deformation of the drawn wire is more and more severe, but also the deformation is gradually extended to the core of the wire.

Figure 10 shows the strain distribution in the drawing deformation zone of micro copper wire during three-pass continuous drawing. From the diagram, it can be seen that the strain distribution inside the wire drawing deformation zone is uneven, and high-strain concentration zones appear in individual grains on the upper surface of the wire, while the strain value inside some grains is almost 0. Not only the strain state inside different grains is different but also the strain distribution in different regions of the same grain is different, which is caused by the orientation and position differences between different grains. With the drawing process, some horizontal strain concentration bands appear in some grains inside the drawn wire. These strain bands are not evenly distributed inside the grains, but appear dispersed distribution. This phenomenon occurs because the grains inside the wire are mostly surrounded by adjacent grains, and the deformation of a single grain must be coordinated with the surrounding grains. In order to maintain the coordination and continuity of inter-grain deformation in a certain area, high strain concentration areas and shear strain bands appear inside the wire. With the increase in drawing passes, the accumulated deformation inside the wire increases. Not only the strain value inside the drawing deformation zone of the wire is gradually increased but also the number

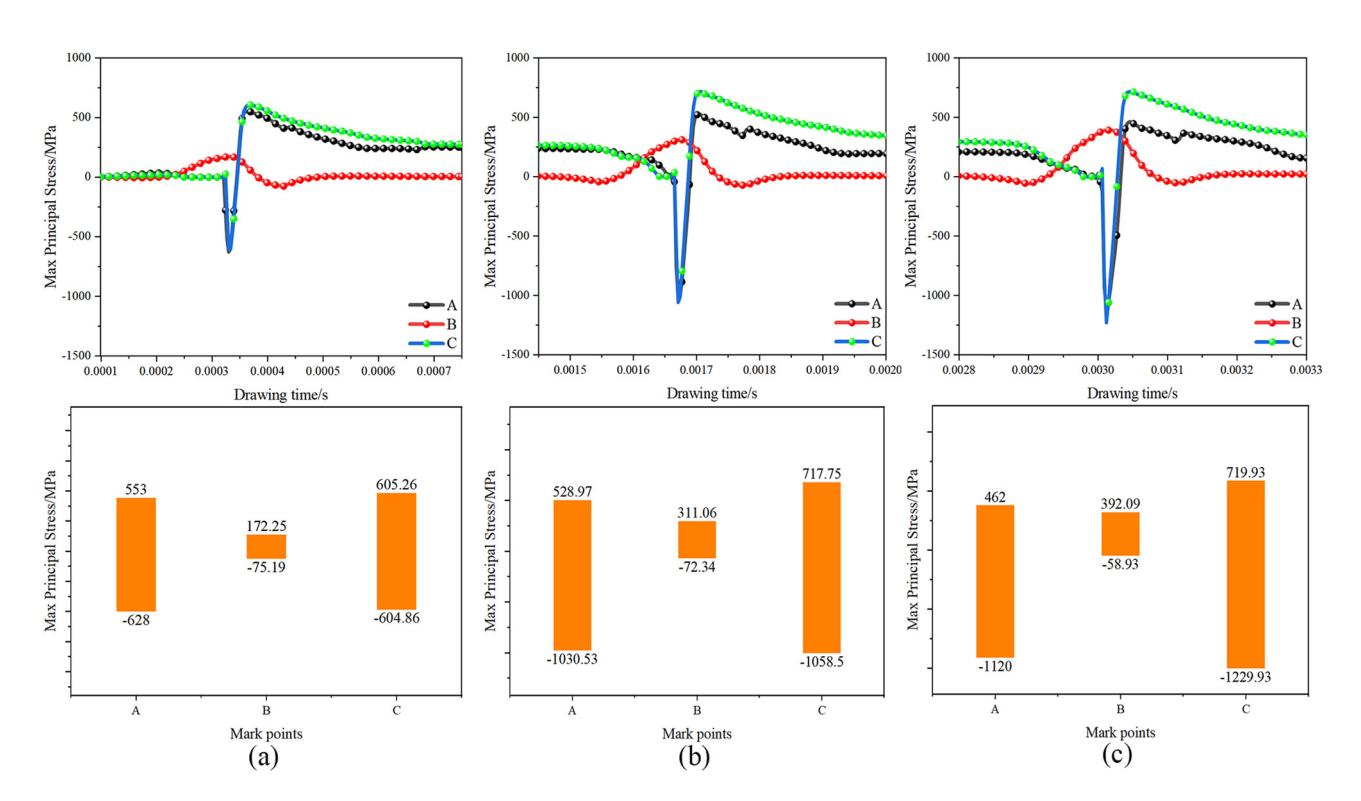


Figure 9: The relationship between the stress of the marked points in the drawing deformation zone and the drawing time in different passes: (a) one pass, (b) two passes, and (c) three passes.

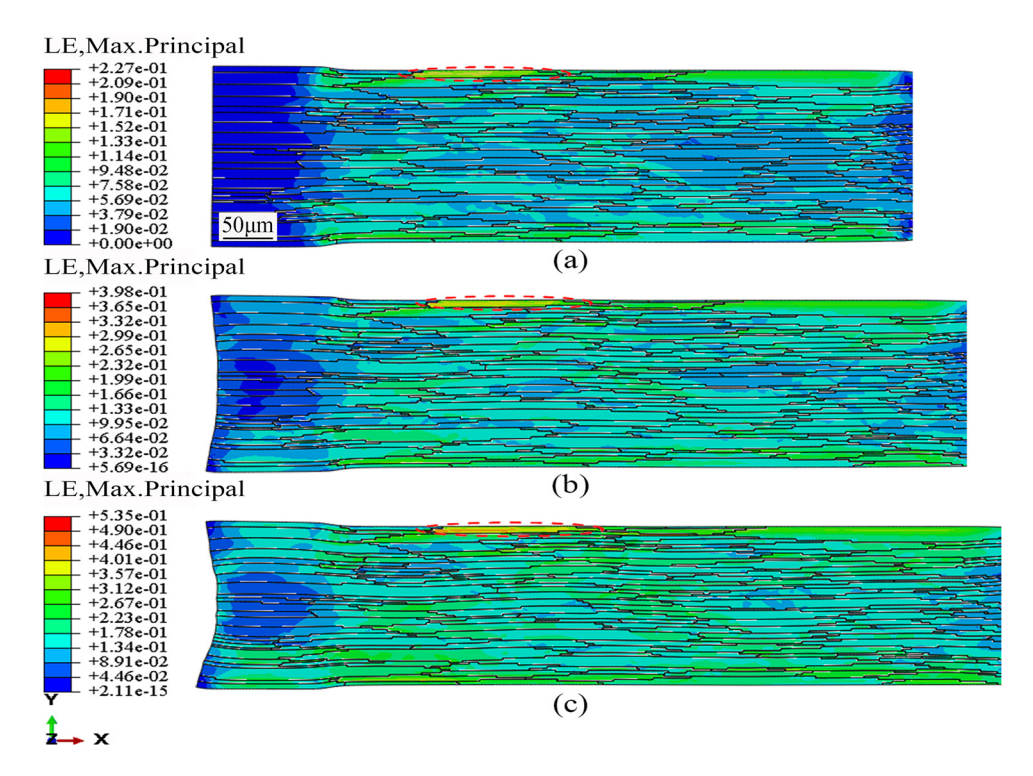


Figure 10: The strain distribution in the drawing deformation zone of wire in different passes: (a) one pass, (b) two passes, and (c) three passes.

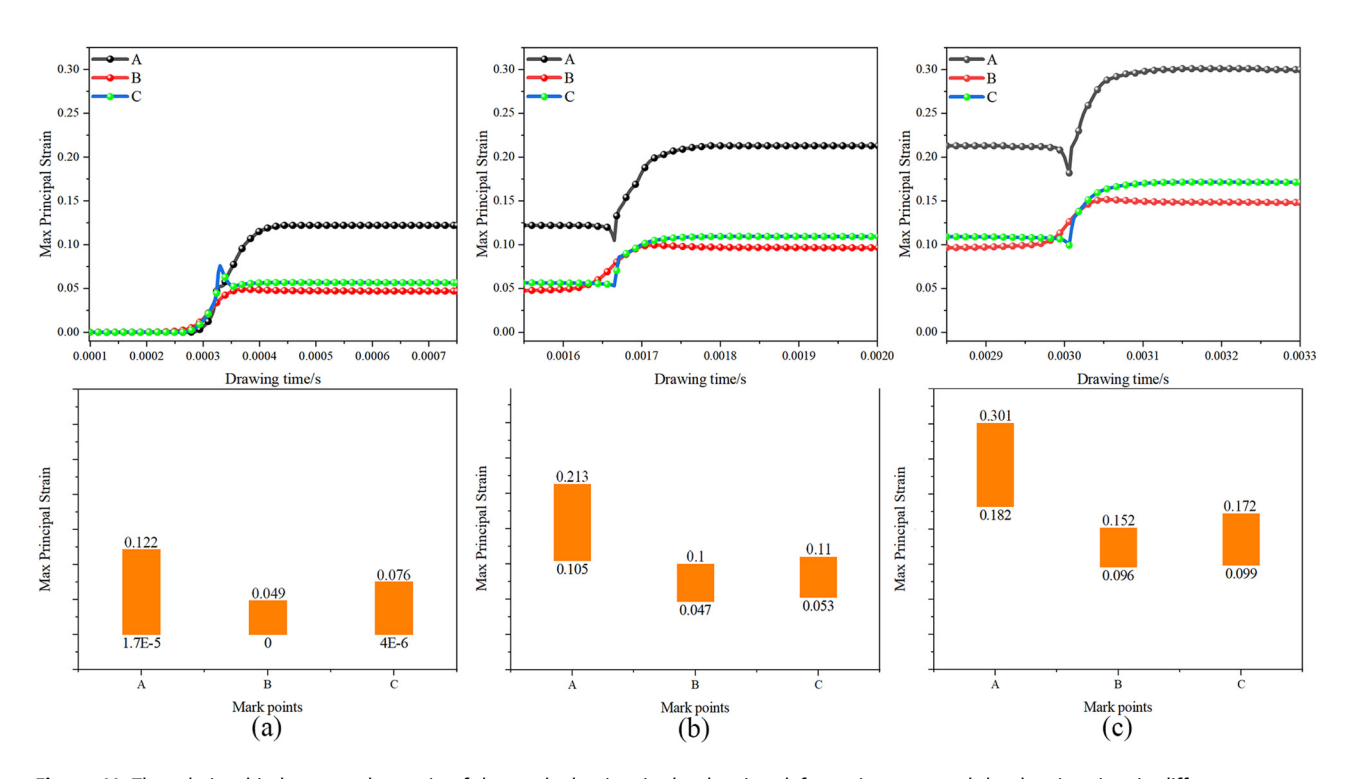


Figure 11: The relationship between the strain of the marked points in the drawing deformation zone and the drawing time in different passes: (a) one pass, (b) two passes, and (c) three passes.

of strain bands inside the wire is obviously increased. The area of the non-deformed zone has also been greatly reduced, indicating that the degree of deformation homogenization has been improved. Figure 11 shows the relationship between the strain of the mark point in the drawing deformation zone of the micro copper wire and the drawing time during the three-pass continuous drawing process. From the diagram, it can be seen that the strain states at different positions inside the wire are quite different during the drawing process. Before the drawing deformation begins, the strain value inside the wire is 0. When a point inside the wire begins to deform, the strain value of the point increases continuously and remains constant after reaching the maximum strain at the point during the later deformation stage of the same drawing pass. With the increase in drawing passes, the strain values at different positions inside the longitudinal section of the drawn wire are increasing. Overall, the strain value of the upper and lower surface of the wire are greater than the strain value of the core of the wire. The strain value on the upper surface of the wire is obviously greater than that of the lower surface of the wire. This is attributed to the influence of grain orientation, where grains with soft orientation are more prone to deformation. In addition, due to the influence of grain shape and position, the deformation state of the grains inside the wire is uneven, and there is a phenomenon of strain localization. The marking point A on the upper surface of the wire

is just in the strain localization area marked by the red dotted line in Figure 10. Therefore, the strain value on the upper surface of the wire is obviously greater than that on the lower surface, which is consistent with the strain distribution of the wire depicted in Figure 10.

Figure 12 shows the cumulative slip distribution in the drawing deformation zone of micro copper wire during three-pass continuous drawing process. SDV121 in the cloud diagram represents the cumulative slip. The drawing process of copper wire is the result of the combined action of 12 slip systems of face centered cubic metal, and the cumulative slip is the sum of the contribution of all slip systems to deformation. From the diagram, it can be seen that the cumulative slip distribution inside the wire is uneven, and the slip area and the non-slip area appear inside the wire. The cumulative slip of each pass is mainly located on the surface of the wire, indicating that the deformation of the grain on the surface of the wire is very severe during the drawing process under the current deformation degree. For different grains on the surface or core of the wire, the cumulative slip distribution is also different. The cumulative slip inside some grains in the core of the wire is almost 0, indicating that these grains have basically not undergone deformation, and also indirectly reflects the anisotropic state of different grains inside the wire. The distribution of cumulative slip in different regions of the same grain is also different. Some grains in the upper and lower surface of

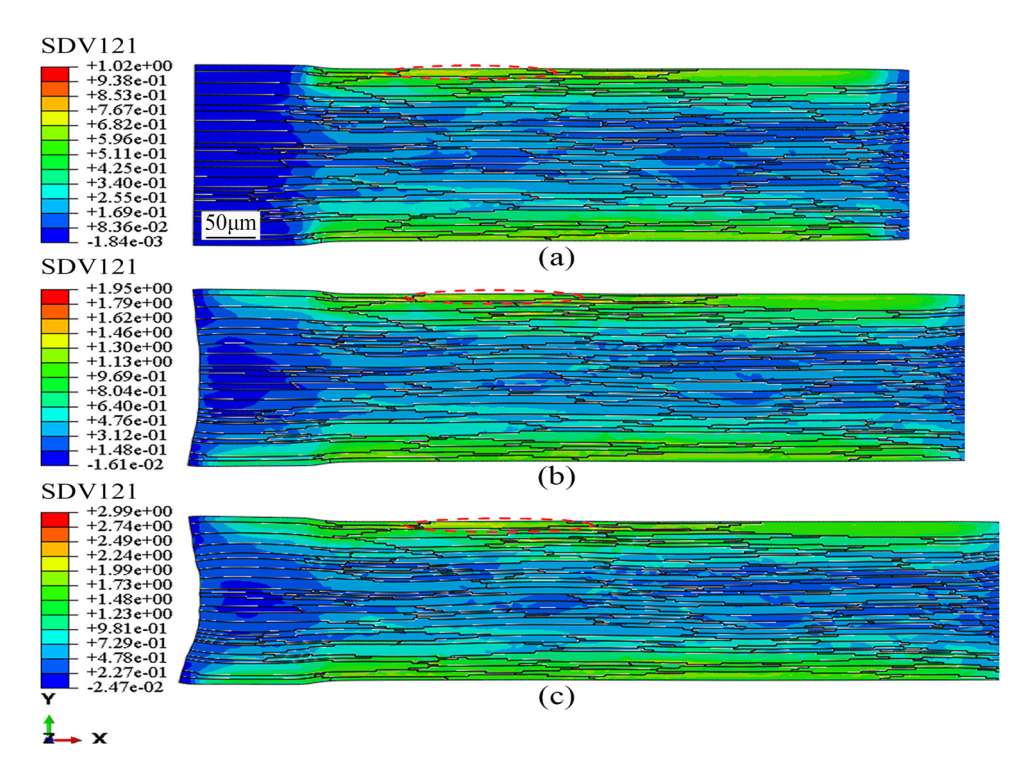


Figure 12: The cumulative slip distribution of wire drawing deformation zone in different passes: (a) one pass, (b) two passes, and (c) three passes.

the wire in direct contact with the drawing die have slip concentration areas as shown in the yellow area, and the localization of slip occurs. With the increase in drawing passes, the cumulative slip inside the wire also continuously increases, and the slip deformation of some grains in the core of the wire is gradually activated.

Figure 13 shows the shear strain distribution of the partial slip system of the wire during stable drawing stage of each pass. SDV14, SDV18, SDV21, and SDV23 represent the shear strain of four main activated slip systems, a2, b3, c3,

and d2, respectively. From the diagram, it can be seen that the shear strain distribution inside the wire and grain is different and uneven for different slip systems. The distribution of each slip system in different wire diameters and different regions within the same wire diameter is also very different. In the same grain, the activation of different slip systems is different, and the motion state of the same slip system in different grains is also different. This is because the grains with initial orientation of soft orientation are prone to deformation, while the grains with initial

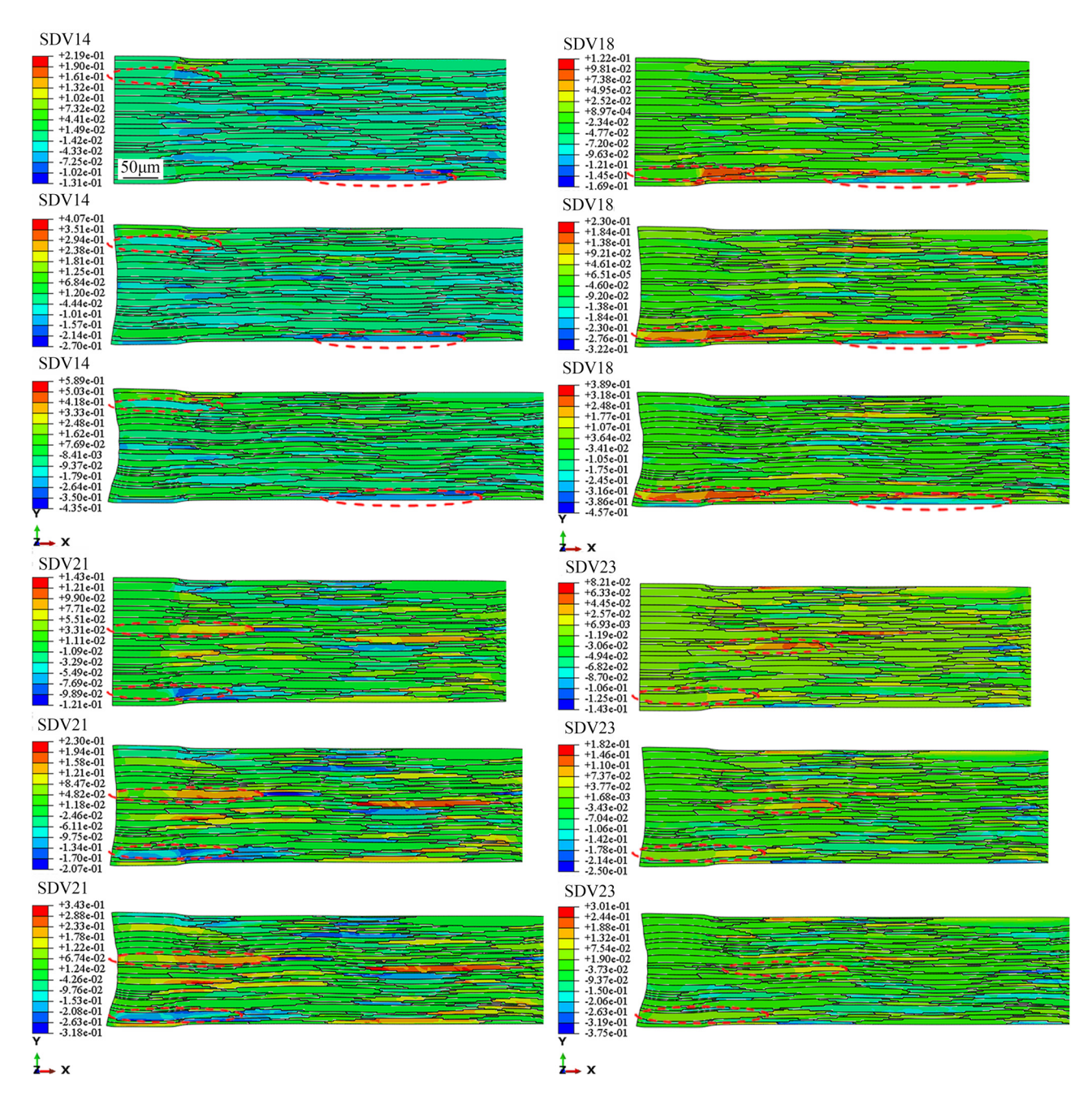


Figure 13: The shear strain distribution of slip systems in the drawing deformation zone of wire in different passes.

orientation of hard orientation are not prone to deformation. The grains on the surface of the wire are directly in contact with the drawing die and bear a greater force, while the grains in the core of the wire are not in contact with the drawing die and bear a smaller force. It is precisely because of the different orientation and position of each grain inside the wire, the deformation degree between each grain during the drawing deformation process of the wire varies greatly, leading to the uneven distribution of shear strain inside the material. From the shear strain cloud diagram, it can be seen that the shear strain inside the drawn wire can be divided into positive and negative values, which represent the two directions of slip motion. The positive value of shear strain indicates that the slip moves in the positive direction, while the negative value is the opposite. With the multi-pass continuous drawing process of the wire, the cumulative deformation degree of the wire increases continuously, the wire diameter decreases gradually, and the grains inside the

wire are obviously elongated. In addition, when the drawing passes increases, the shear strain values of each slip system inside the wire also continuously increase, and the maximum shear strain area of the activated slip system gradually expands and increases inside the grain. It shows that with the increase in deformation passes, the degree of deformation homogenization inside the grains is improved, which also reflects the structure inheritance of the wire during multipass continuous drawing to a certain extent. The so-called structure inheritance refers to the inheritance law of microstructure characteristics of material in continuous material processing. By analyzing the structure inheritance, we can better understand the microstructure evolution of wire.

For the multi-pass continuous drawing process of wire, the relationship between the shear strain and drawing time of each slip system at positions A, B, and C of the wire drawing deformation zone is shown in Figure 14. The positions of the three markers A, B, and C are located on the upper surface, core, and lower surface of the wire

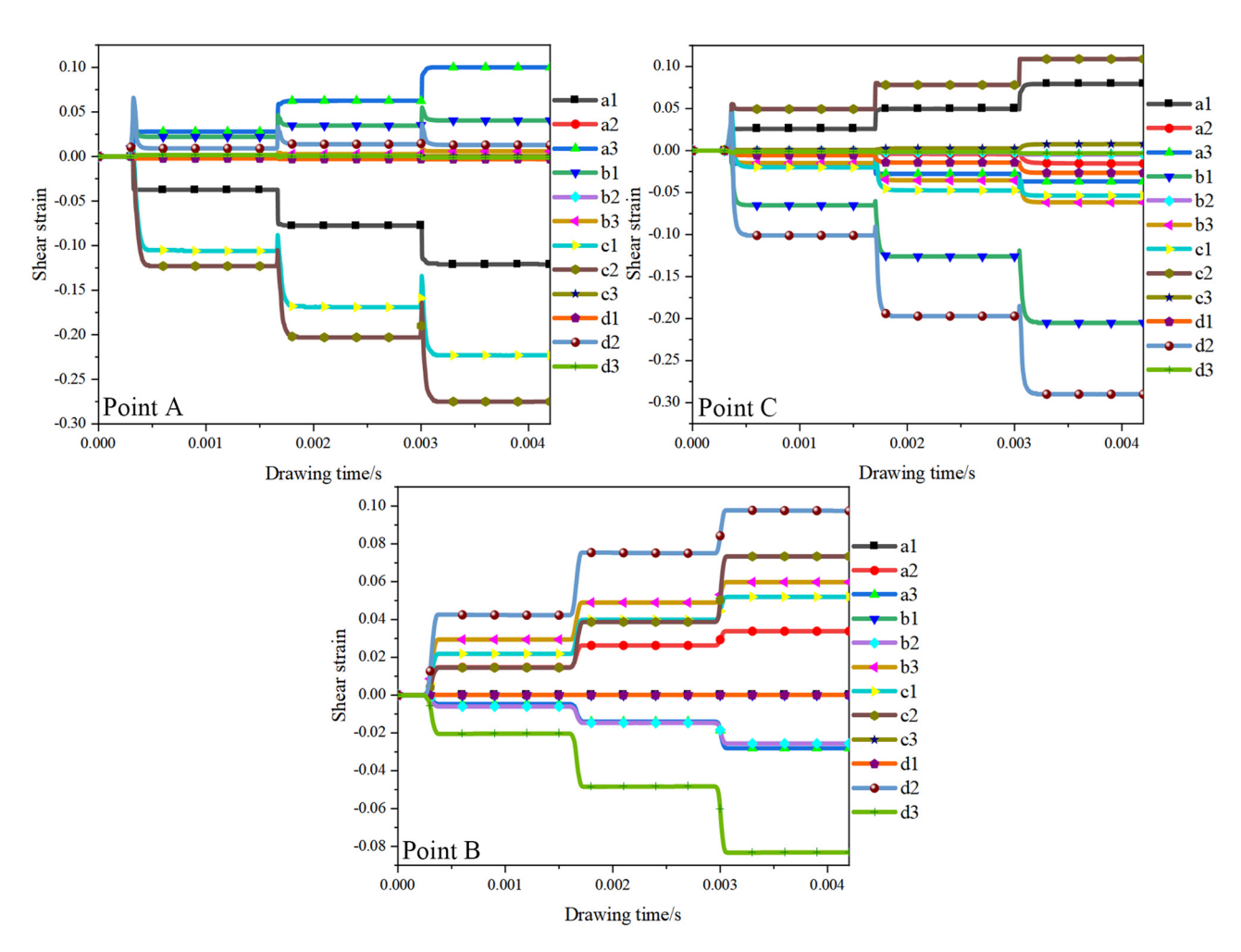


Figure 14: The relationship between the shear strain and drawing time of each slip system at positions A, B, and C of the wire drawing deformation zone.

drawing deformation zone, respectively, reflecting the activation and movement of the slip systems at each position. The activation of the slip systems can be reflected by the size of shear strain, with higher shear strain indicating more significant activation of the slip system, while shear strain of 0 indicates that the slip system is not activated. It can be seen from the diagram that the slip is quickly initiated after the wire enters the drawing deformation zone. The types and motion states of the activated slip systems at different positions inside the wire in the drawing deformation zone are different, and the three marker points are all in a state of multiple slip systems activation. Some slip systems are obviously activated, such as the significant contribution of the c2 slip system at point A on the upper surface, and the maximum contribution of the d2 slip system at point B in the core and point C on the lower surface. Some slip systems are hardly activated during one-pass drawing,

and these slip systems are obviously activated after two-pass drawing. Some slip systems are not activated throughout the continuous drawing process. In general, the shear strain on the upper and lower surfaces of the wire is significantly larger than that in the core, explaining that the deformation degree of the wire surface is larger than that in the core under the direct action of the drawing die. With the increase in deformation passes, the shear strain of each slip system continuously increases, which is consistent with the conclusion drawn in Figure 13. The significant fluctuation of shear deformation in the slip systems b1, d2, c1, and c2 at upper surface point A and b1 and d2 at lower surface point B during the wire drawing process indicates that the variation in drawing passes has a greater impact on the shear deformation of the upper and lower surfaces of the drawn wire.

Figure 15 shows the changes in the (111) pole diagrams of G197, G78, and G163 grains inside the wire before and

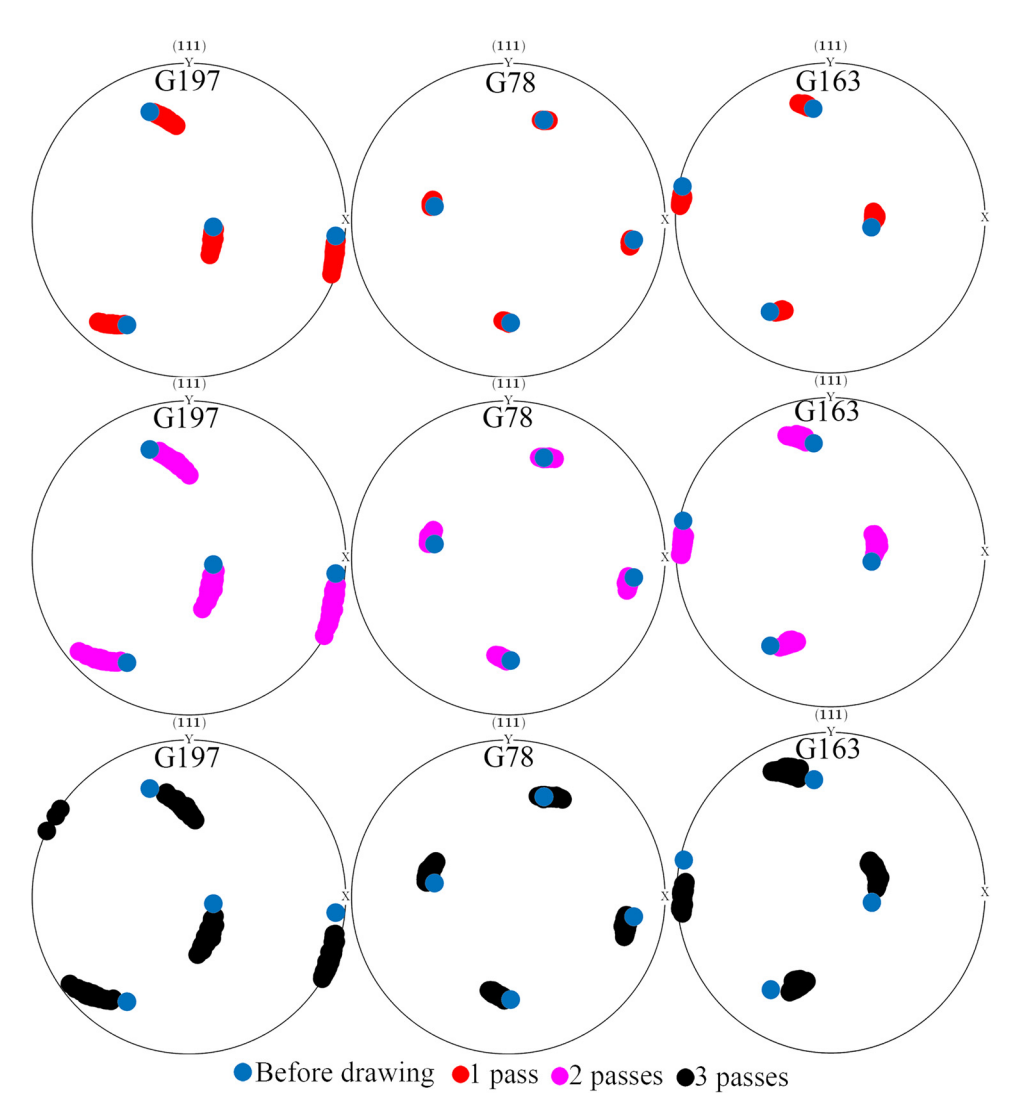


Figure 15: (111) pole figure of G197, G78, and G163 grains before and after deformation.

after drawing deformation in different passes. G197, G78, and G163 grains, respectively, represent the grains on the upper surface, core, and lower surface of the wire. The blue dots represent the initial orientation of the grains before deformation, while the red dots, cyan purple dots, and black dots represent the orientation of the grains after one-pass, two-pass, and three-pass drawing deformation, respectively. From the diagram, it can be seen that the initial orientations of different grains inside the wire before deformation are different and the orientation poles are centrally distributed in the pole diagram. After deformation of the grains, the concentrated orientation poles are dispersed. The orientation poles of each grain are rotated by a certain angle around the Z axis and are dispersed around the initial orientation. This rotation angle is temporarily defined as dispersion. With the drawing deformation, the deformed G197, G78, and G163 grains rotate obviously around the Z axis, and the rotation angle of each grain varies greatly due to the different positions and initial orientations of the grains. In addition, the upper surface grain G197 and the core grain G78 rotate clockwise, and the lower surface grain G163 rotates counterclockwise. The rotation direction of different grains after deformation is also different. After one pass of drawing deformation, the rotation angle and dispersion of the orientation poles of the upper surface grain G197 and the lower surface grain G163 are significantly larger than that of the core grain G82. From the stress and strain cloud diagram, it can be seen that the grain G197 is obviously located in the region of stress and strain concentration, so its rotation angle and dispersion are the largest among the three grains. With the increase in drawing passes, the rotation angle of grains and the dispersion of orientation poles increase obviously, and the position of orientation poles with dispersed distribution is shifted in the XY plane compared with the initial orientation. When the drawing deformation reaches the third pass, a new orientation pole appears in the polar figure of the upper surface grain G197 after deformation. This reflects that sub-grains are formed in the surface grains of the wire after continuous cumulative deformation of three drawing passes, under the sustained effect of high stress and strain, so a new orientation pole is projected in the pole figure.

5 Conclusion

The crystal plasticity finite element model of three-pass continuous drawing process of pure copper micro wire under the same wire diameter compression ratio was established, and the reliability of the model was proved. The effect of drawing passes on the continuous drawing deformation of pure copper micro wire at meso-scale is mainly discussed. The conclusions are as follows:

- 1) The stability of the high-speed continuous drawing process of micro copper wire and the surface quality of the drawn wire are affected by the interaction between the drawing force and contact stress occurring between the drawing die and the wire. With the increase in deformation passes, the fluctuating drawing force and contact stress lead to a decrease in the deformation stability of the continuous drawing process of the wire.
- 2) The internal deformation of the wire during the continuous drawing process is not uniform, and there is a phenomenon of local large deformation. There is a fracture risk zone under the alternating action of positive and negative stress values in the deformation zone of the drawn wire. The stress, strain, and cumulative slip of the wire drawing deformation zone gradually increase with the increase in the drawing passes.
- 3) With the increase in deformation passes, the shear strain of each slip system continues to increase, and the deformation uniformity inside the grains is improved. The effect of the drawing die on the surface grains and the core grains of the wire is different, leading to different types of activated slip systems and motion states in the grains at different positions. The change in drawing passes leads to the obvious activation of some inactivated slip systems, which has a greater influence on the shear deformation of the surface of the drawn wire.
- 4) The rotation direction of different grains in the drawn wire is different after deformation. The rotation angle and dispersion of the orientation poles of the surface grains are significantly larger than those of the core grains. With the increase in drawing passes, this trend is more obvious.

Funding information: This work was supported by the National Natural Science Foundation of China (U21A2051, 52173297, 52071133), R & D Projects of Henan Academy of Sciences (220910009), Key R & D and Promotion Projects of Henan Province (212102210441), and Zhongyuan scholar workstation funded project (214400510028).

Author contributions: All authors have accepted responsibility for the entire content of this manuscript and approved its submission.

Conflict of interest: The authors state no conflict of interest.

References

- Zhang P, Zhou Y, Liu Y, Li S, Song K, Cao J, et al. Strengthening mechanism of ultra-high strength Cu-20Ag alloy wire induced by cumulative strain. Mater Sci Eng A. 2022;855:143957.
- Sun PF, Zhang PL, Hou JP, Wang Q, Zhang ZF. Quantitative mechanisms behind the synchronous increase of strength and electrical conductivity of cold-drawing oxygen-free Cu wires. J Alloy Compd. 2021;863:158759.
- Zidani M, Messaoudi S, Dendouga F, Baudin T, Derfouf C, Boulagroun A. et al. Multi-scale analysis by SEM, EBSD and X-ray diffraction of deformation textures of a copper wire drawn industrially. Matec Web Conf. 2013;5:1-3.
- Hanazaki K, Shigeiri N, Tsuji N. Change in microstructures and mechanical properties during deep wire drawing of copper. Mater Sci Eng A. 2010;527:5699-707.
- Yang F, Dong L, Cai L, Wang L, Xie Z, Fang F. Effect of cold drawing strain on the microstructure, mechanical properties and electrical conductivity of low-oxygen copper wires. Mater Sci Eng A. 2021;818:141348.
- Chen DC, Huang JY. Design of brass alloy drawing process using Taguchi method. Mater Sci Eng A. 2007;464:135-40.
- Chang CC, Hsieh TY, Kao HC, Shao SY, Hsu CH. Prediction of hardness in drawn copper wire by effective strain from finite element simulation. Mater Sci Forum. 2019;947:103-8.
- Celentano JD. Thermomechanical simulation and experimental validation of wire drawing processes. Mater Manuf Process.
- [9] Tang KK, Li ZX, Wang J. Numerical simulation of damage evolution in multi-pass wire drawing process and its applications. Mater Design. 2011;32:3299-311.
- [10] Arya A, Suwas S, Gerard C, Signor L, Thilly L, Chokshi AH. Strength and microstructure evolution in nickel during large strain wire drawing. Acta Mater. 2021;221:117396.
- [11] Chen JX, Chen Y, Liu JP, Liu TW, Dai LH. Anomalous size effect in micron-scale CoCrNi medium-entropy alloy wire. Scripta Mater. 2021;199:113897.
- [12] Guo S, He Y, Li Z, Lei J, Liu D. Size and stress dependences in the tensile stress relaxation of thin copper wires at room temperature. Int J Plast. 2019;112:278-96.
- [13] Guo S, He Y, Tian M, Liu D, Li Z, Lei J, et al. Size effect in cyclic torsion of micron-scale polycrystalline copper wires. Mater Sci Eng A. 2020;792:139671.
- [14] Juul KJ, Nielsen KL, Niordson CF. Steady-state numerical modeling of size effects in micron scale wire drawing. J Manuf Process. 2017;25:163-71.

- [15] Zhu YK, Chen QY, Wang Q, Yu HY, Li R, Hou JP, et al. Effect of stress profile on microstructure evolution of cold-drawn commercially pure aluminum wire analyzed by finite element simulation. J Mater Sci Technol. 2018;34:1214-21.
- [16] Yang MX, Luan TJ, Zhou TG, Zhang XF. Computer simulation of aluminum conductors drawn in high speed. Adv Mater Res. 2013;834:1567-70.
- [17] Jian CH, Wen YA, Wei LI, Jian MI, Fan XH. Texture evolution and its simulation of cold drawing copper wires produced by continuous casting. T Nonferr Metal Soc. 2011;21:152-8.
- Sun LX, Bai J, Xue F. Evolutions of microstructure and texture of Mg-Gd alloy wires processed by cold drawing. J Mater Res Technol. 2022:21:3961-9.
- [19] Wang M, Yang Q, Jiang Y, Qin L, Tan F, Xin Z, et al. Microstructure evolution and mechanical property of directionally solidified Cu-9Ni-6Sn alloy wire during aging. J Mater Res Technol. 2022;21:474-85.
- [20] Amelirad O, Assempour A. Experimental and crystal plasticity evaluation of grain size effect on formability of austenitic stainless steel sheets. J Manuf Process. 2019;47:310-23.
- [21] Taylor GI. The mechanism of plastic deformation of crystals. Part I —theoretical. P Roy Soc A-Math Phy. 1997;145:362-87.
- [22] Taylor GI. The mechanism of plastic deformation of crystals. Part II.—comparison with observations. P Roy Soc A-Math Phy. 1997;145:388-404.
- [23] Asaro RJ, Needleman A. Overview no. 42 Texture development and strain hardening in rate dependent polycrystals. Acta Metall. 1985:33:923-53.
- Peirce D, Asaro RJ, Needleman A. Material rate dependence and [24] localized deformation in crystalline solids. Acta Metall. 1983;31:1951-76.
- [25] Kalidindi SR, Bronkhorst CA, Anand L. Crystallographic texture evolution in bulk deformation processing of FCC metals. I Mech Phys Solids. 1992;40:537-69.
- [26] Hill R, Rice JR. Constitutive analysis of elastic-plastic crystals at arbitrary strain. J Mech Phys Solids. 1972;20:401-13.
- [27] Chen SD, Liu XH, Liu LZ. Symmetric and asymmetric rolling pure copper foil: Crystal plasticity finite element simulation and experiments. Acta Metall Sin-Engl. 2015;28:1024-33.
- [28] Lu X, Zhang X, Shi M, Roters F, Kang G, Raabe D. Dislocation mechanism based size-dependent crystal plasticity modeling and simulation of gradient nano-grained copper. Int J Plast. 2019;113:52-73.
- [29] Zeng B, Wu J, Zhang H. Numerical simulation of multi-pass rolling force and temperature field of plate steel during hot rolling. J Shanghai Jiaotong Univ (Sci). 2011;16:141-4.